Lessons Learned in the Flight Qualification of the S-NPP and NOAA-20 Solar Array Mechanisms

Daniel Helfrich* and Adam Sexton**

Abstract

Deployable solar arrays are the energy source used on almost all Earth orbiting spacecraft and their release and deployment are mission-critical; fully testing them on the ground is a challenging endeavor. The 8 meter long deployable arrays flown on two sequential NASA weather satellites were each comprised of three rigid panels almost 2 meters wide. These large panels were deployed by hinges comprised of stacked constant force springs, eddy current dampers, and were restrained through launch by a set of four releasable hold-downs using shape memory alloy release devices. The ground qualification testing of such unwieldy deployable solar arrays, whose design was optimized for orbital operations, proved to be quite challenging and provides numerous lessons learned. A paperwork review and follow-up inspection after hardware storage determined that there were negative torque margins and missing lubricant, this paper will explain how these unexpected issues were overcome. The paper will also provide details on how the hinge subassemblies, the fully-assembled array, and mechanical ground support equipment were subsequently improved and qualified for a follow-on flight with considerably less difficulty. The solar arrays built by Ball Aerospace Corp. for the Suomi National Polar Partnership (S-NPP) satellite and the Joint Polar Satellite System (JPSS-1) satellite (now NOAA-20) were both successfully deployed on-obit and are performing well.

Introduction

One of the first key events on larger spacecraft is the mission-critical deployment of the solar array, providing electrical power collection capability to sustain the mission for its duration. Prior Ball Aerospace satellites used smaller solar arrays that could stow around the body of the satellite structure. Embarking on a new design effort required the design and qualification of new solar array mechanisms, composite panels to support solar cells (substrates) and the ground test equipment. During the S-NPP lifecycle the new mechanisms encountered design and test issues, which included excessively stacked constant torque springs, incorrectly processed parts, variable resistive torque profile through the range of motion of the hinge, unplanned resistive torques, inadequate harness characterization, inability to complete subsystem level vibration testing and issues with subsystem level deployments. Design flaws identified from the S-NPP program were addressed during the JPSS-1 program and provided for much smoother delivery of mechanisms to the subsystem assembly, however lingering issues with the gravity-negation deployment system design and usage in different configurations provided some new challenges to overcome.

Sources of Driving Mechanisms Requirements

The solar array for S-NPP was required to be compliant with MIL-A-83577B, “Moving Mechanical Assemblies for Space Launch Vehicles (MMA),” and with the GEVS standard, an acronym for Goddard Environmental Verification Standard, GSFC-STD-7000. Both require margins on the driving torques to assure robust mechanism performance. GEVS mandates the use of factors of safety on the sources of

* NASA Goddard Space Flight Center, Greenbelt, Maryland
** Ball Aerospace Corporation, Boulder, Colorado

drag torque in completing the analysis. When JPSS-1 began, the standard known as the "Gold Rules," GSFC-STD-1000, was also implemented, driving the project towards more rigorous solar array testing. Because of the extreme difficulty of implementing full solar array tests in compliance with the Gold Rules, most large solar array testing has to be scaled back via a waiver.

S-NPP Solar Array Development

Figure 1 shows the S-NPP and JPSS-1 satellites with their highly similar solar arrays deployed, showing their zenith-facing and Earth-facing sides, respectively. Three solar panels are tied together by two inter-panel hinge (IPH) lines consisting of a passive and powered hinge and a main deployment hinge (MDH) at the interface between the inner panel and the rotational drive assembly (RDA), which tracks the sun. Each of the powered hinge lines are driven by a constant torque spring and rate controlled with eddy current dampers.

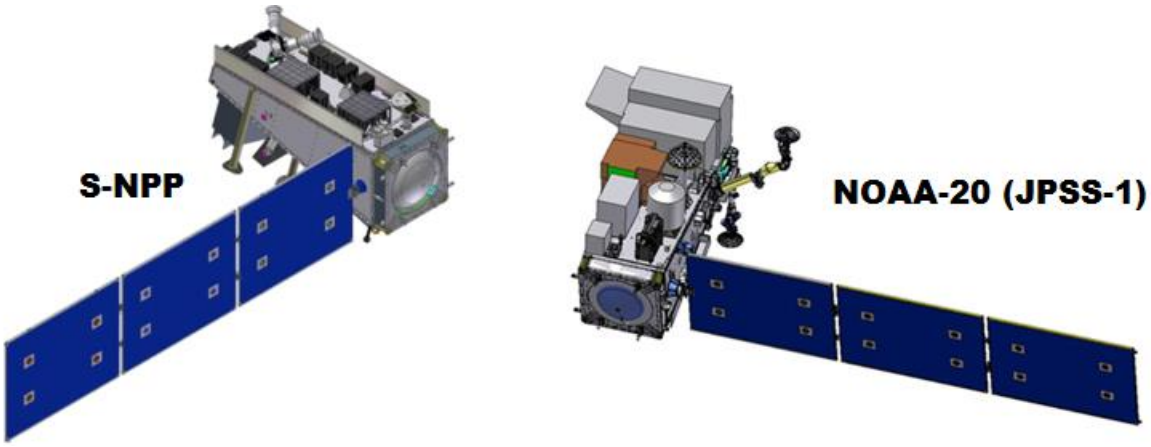

Figure 1. S-NPP and JPSS-1 Satellites (Fully-deployed)

Hinge Torque Margin Troubles

The solar array for S-NPP was designed to be compliant with the MMA requirements in the beginning of the program showing large torque ratios, but as the program reached the testing phase and the use of the GEVS torque margin analysis was followed, difficulties arose in meeting required torque margins. There were multiple issues that drove torque margins negative which is explored below. Early in the design phase, the torque margins were required to be greater than zero using phased factors of safety applied to the sum of known torques (ΣT_K) and unknown torques (ΣT_U) according to the following formula:

$$Torque\ Margin = \left[\left\{\frac{Torque\ Available}{(FS_K \cdot \Sigma T_K + FS_U \cdot \Sigma T_U)}\right\} - 1\right] \text{ must be} > 0.0$$

Table 1 GEVS Factors of Safety through program life

Program Phase	Known Torque Factor of Safety (FS_K)	Variable Torque Factor of Safety (FS_V)
Preliminary Design Review	2.00	4.0
Critical Design Review	1.5	3.0
Acceptance/Qualification Test	1.25	3.0

Typical known resistive torque are things like inertia, or magnetic coulomb friction and unknown resistive torques are things like friction within the mechanism or the resistive torque of a harness.

Torque margin analysis matured through the design of the hinges and into the test program. The initial revision of the torque margin analysis, in 2003, was determined using analytical values for resistive torques and used the Critical Design Review (CDR) factors of safety from Table 1 and shown in Table 2. IPH1 is the hinge line closest to the spacecraft body. Revision A of the analysis was an update based on initial testing of the hinges and the supporting harness as well as measured values for damper resistive torques. After it was measured, the harness resistive torque changed from an anticipated value of 0.5 in-lb to a value of 3.2 in-lbs for the IPH. The MDH harness resistive torque changed from an anticipated value of 2 in-lbs to a measured value of 1.5 in-lbs. This analysis used the Acceptance/Qualification Test factors of safety shown in Table 3. Revision B accounted for a requested change to analyze the margin based on the factors of safety shown in Table 1. Revision C of the analysis addressed a reduction in the available torque of the system which was reduced and a change in the factors of safety. The IPH was calculated using CDR values from Table 3 and the MDH was determined using Acceptance/Qualification values from Table 3. Values of available torque were found between 2004 and 2005 with a torque watch and did not provide an accurate torque versus angle measurement and minimum and maximum available torques were not available.

Table 2 Change in Margin during S-NPP

Hinge Type	Rev -	Rev A	Rev B	Rev C	Pre S/C Integration	Pre-Ship Torque Margin	Pre-Ship Torque Ratio
IPH1	0.695	0.791	0.361	0.279	0.067	-0.016	1.58
IPH2	0.695	0.791	0.361	0.279	0.067	0.06	1.94
MDH	0.306	0.780	0.439	0.780	0.09	-0.22	1.48
IPH Torque – known (in-lbs)	6.496	5.756	5.756	5.756	6.424	4.98 (IPH 1) 5.55 (IPH 2)	
IPH Torque – variable (in-lbs)	5.406	11.32	11.32	11.32	10.65	15.25 (IPH 1) 10.50 (IPH 2)	
IPH available torque (in-lbs)	44	56	56	40	33	31.9 (IPH 1) 31.1 (IPH 2)	
MDH Torque – known (in-lbs)	12.33	11.37	11.37	11.37	7.87	7.85	
MDH Torque – variable (in-lbs)	7.62	13.1	13.1	13.1	16.60	33.1	
MDH Available torque (in-lbs)	54	77	77	77	49	60.5	
FS known	1.5	1.5	1.25	1.5	1.5	1.5	
FS unknown	3.0	2.0	3.0	2.0	2.0	2.0	

In 2009, after hardware storage, concerns were raised about the variability of output torques in the hinges and it was determined that better characterization of the hinge lines was required. IPH testing was carried out to measure the output torque across the full range of motion in both directions and found that the available torque dropped from previously measured values. It also found that the resistive torque from the pawl was variable due to the cam shape of the hinge. The MDH was also recharacterized and again the minimum torque measured during the range of motion resulted in a significant drop in the torque margin at S/C pre-integration.

Table 3 Updated Margin values

Program Phase	Known Torque Factor of Safety (FS_K)	Variable Torque Factor of Safety (FS_V)
Preliminary Design Review	2.00	4.0
Critical Design Review	1.5	3.0
Acceptance/Qualification Test	1.5	2.0

To remain consistent with prior NASA Goddard practice, torque resistances were updated using the more conservative "Zero-Neutral" approach for characterization of the harnesses, wherein the net resistance is the sum of the worst case deploying torque at beginning of rotation plus the worst-case stowing torque at the end of rotation. The use of non-flight harness in tests also arose as an issue because of the natural variability of wire geometry within their respective harnesses. Without photographic or other proof that the original test harnesses were essentially the same, re-testing of freshly built flight-like harnesses was mandated. This testing measured the actual harness route of the RDA and compared it to the test harness that was built. The results of this testing showed that the test harness matched the behavior of the flight harness. The "Zero-Neutral" approach changed the resistive torque characterization of the harness value from a resistive torque of 1.5 in-lbs used from the harness testing done in 2004 to 20 in-lbs. The IPH1 hinge line harness resistance values were changed from 2.0 in-lbs to 6.7 in-lbs. IPH2 hinge line values were updated to 3.3 in-lbs. The changes in these harness values and applying the required factors of safety drove the torque margins to negative values reported in Table 2.

During the 2009 investigation on the characterization of the torque output of the hinges it was found that the constant torque springs were developing an unintended gap, shown in the right side of Figure 2. The gap signals too much frictional losses in the spring stack. A wet lubricant, Braycote 601VB, was applied to the both the roller and the spring stack to reduce friction and torque resistance. The roller shaft that should have been dry lubricated was found to be unprocessed, so a grease plate mixture of Braycote 601 VB and 30% molybdenum disulfide was applied to it.

Despite the team's best efforts, margins were still negative, and it was too late to redesign. So that required the generation and processing of a waiver. In the waiver, since the torque ratio was higher than 1.0, indicating there was driving torque above the minimum, the negative margins were deemed acceptable based on the extensive and recent testing. This waiver was presented to NASA in mid-August 2011 and the array was successfully integrated 2 days after the waiver was approved.

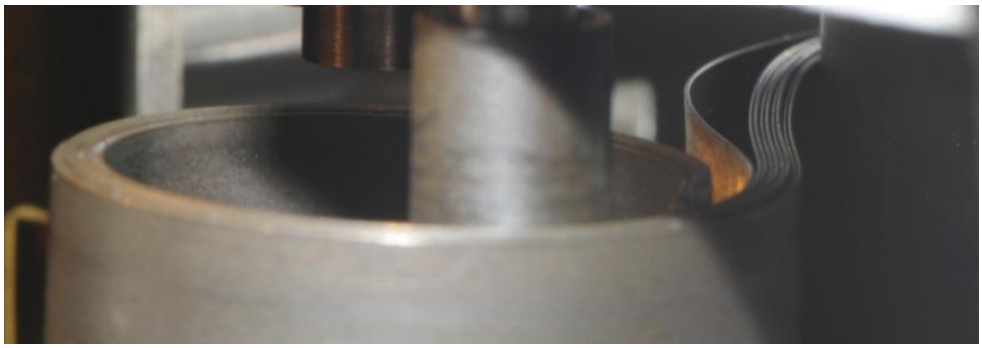

Figure 2. Gapping in the Leaf Spring of the Main Deployment Hinge

Testing the Solar Array

The testing flow for the components and assemblies in the S-NPP solar array was rigorous starting at component level testing for mechanisms, release mechanisms, panel substrates and the solar cells prior to and after attachment to the substrate. After these elements are assembled the entire subassembly

goes through pre-environmental testing, environmental testing and then post-environmental testing. Pre-environmental testing included deployment testing, electrical testing and Large Area Pulsed Solar Simulator (LAPSS) testing. Environmental testing consisted of vibration testing and thermal vacuum testing after which the pre-environmental testing sequence was repeated.

Figure 3 shows the S-NPP solar array when it was tested while attached to the satellite and the arrangement of the gravity-negation ground support equipment (GSE)—also used for array testing when not attached to the satellite. For hardware safety and GSE simplicity, all of the full deployment tests of the S-NPP solar array were conducted on a separate test stand with the array removed from the Rotational Drive Assembly (RDA). Subsystem level deployment testing was a challenge throughout the S-NPP life cycle. The deployment GSE consisted of a number of thick honeycomb panels that were attached to each other to provide a surface that the solar array could be deployed on through the use of air bearings. This configuration presented a number of challenges as at each panel joint there often arose a discontinuity that resulted in the air bearing "dropping out" and the solar array deployment would stop. A number of fixes were attempted to close out this gap and prevent the array from stopping during deployment. The final solution used a continuous, smooth, and flexible roofing material that was laid out over the top of the deployment fixture. This roofing material was a 0.060 thick polyolefin membrane and the resulting smooth table surface is shown in Figure 4.

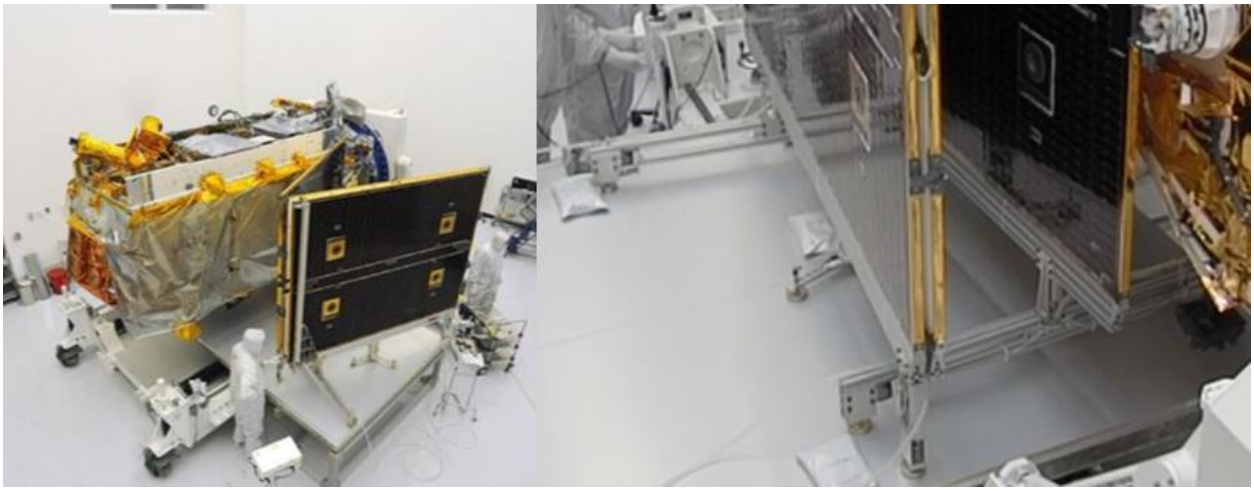

Figure 3. First Motion "Pop and Catch" Testing (Overview and GSE Closeup)

Figure 4. Subsystem deployment testing with Polyolefin membrane topping the raised deployment floor

JPSS-1 Solar Array Development

Ball Aerospace was awarded JPSS-1 as a follow on to S-NPP in September 2010. The architecture of JPSS-1 was to be a "clone" of S-NPP. However, one of the differences that directly impacted the solar array design and accommodation was the inclusion of two TDRSS antennas, one nadir pointing and the other zenith pointing. Figure 5 shows that the nadir pointing antenna was positioned between the bus and the solar array. This forced the solar array to be translated 4 inches further out from the bus panel than on S-NPP. This accommodation was made by incorporating standoff brackets under the four RRS (Retention and Release Subsystem) brackets and under the RDA. JPSS-1 took advantage of new cell technology and transitioned to a new type, the "XTJ," which increased current so that additional wires were required to cross each inner panel hinge line and the main deployment hinge line. Also, on JPSS-1, the Gold Rules were tailored in the mission specific requirements and flowed down to engineering through an Environmental Design and Testing Specification (EDTS).

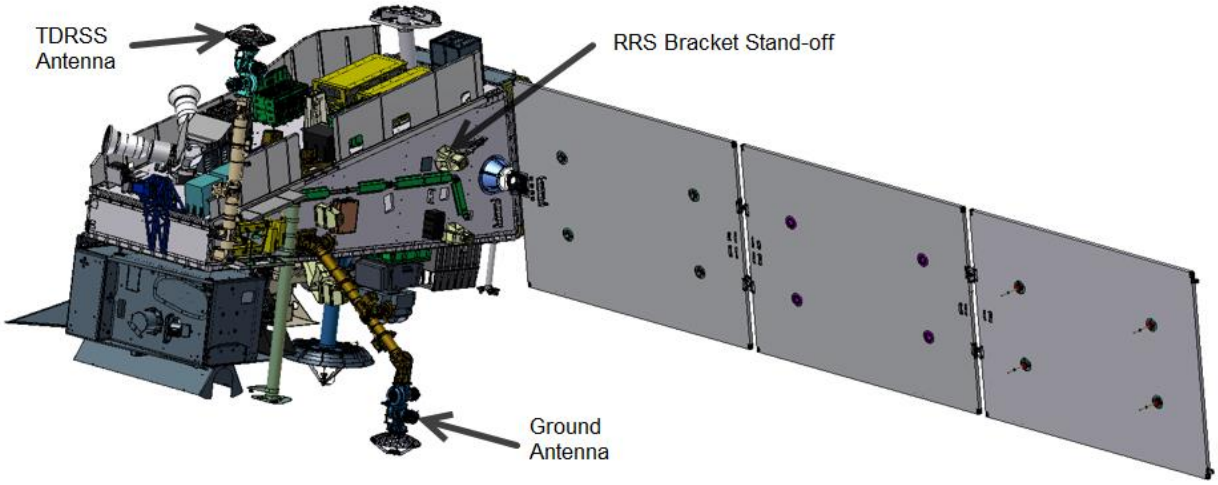

Figure 5. JPSS-1 Observatory (Deployed configuration)

Hinge Design Updates

The issues raised during the S-NPP torque margin investigation were addressed with design updates for JPSS-1. One significant update addressed a "rule of thumb" of the spring vendor to limit the number of springs in a stack to 3. The width and thickness of the springs were made larger to increase their torque and reduce the number needed to meet torque margin requirements. The hinges went through a test program, discussed below, that characterized the drag torques that must be overcome and satisfy the torque margin requirements. JPSS-1 had an increase of 32 wires crossing the MDH hinge line and 7 additional wires crossing each IPH hinge line. The number of springs was determined based on the drag torque characterization testing, then installed on the hinge and characterized over the range of motion.

Referring to Figure 6, the output drum was increased in diameter and arc length to accommodate the large constant torque spring. Two additional fasteners were added for load carrying capability and the ability to add a piece of MGSE that would make manual rotation of the hinge easier and to allow instrumented torque measurements. The change in the spring design required more spacing between the output drum and take up roller. The take up roller diameter was increased to reduce its deflection.

An additional Vespel washer was placed between the end of the roller sleeve and the washer on the end to minimize friction between the roller sleeve and the CRES washer. The MDH axles were changed from the S-NPP design by eliminating cotter pins from the central area of the MDH where the RDA harness routes to the connector bracket on the inner panel. This minimized the amount of sharp edges exposed to the harness. The pawl, not shown, was modified to have a spherical surface that would engage the bottom of the cam surface at the end of range of motion and would provide a point contact during lockout.

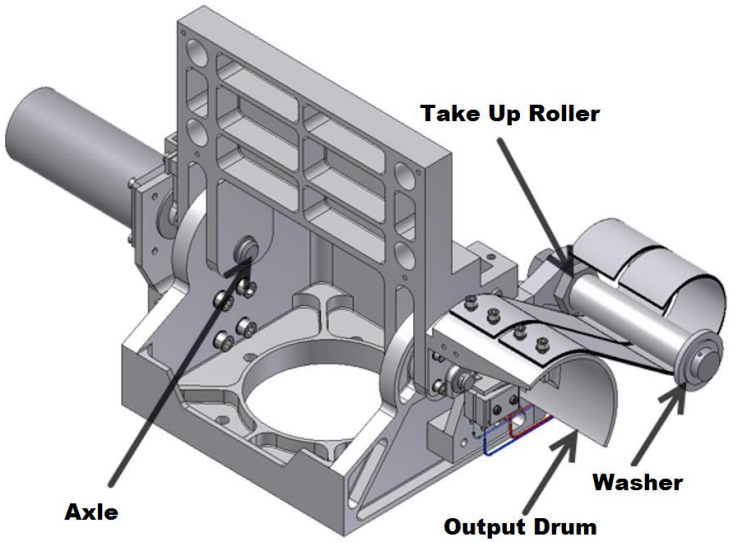

Figure 6. MDH in deployed orientation

This IPH hinge design shown in Figure 7 also went through similar evolutions as the MDH. The output drum was increased in size to accommodate the larger constant torque spring. As with the MDH the take up roller was increased in diameter to minimize the deflection and accommodate the stronger spring sized for JPSS-1. The biggest change for the IPH design was the change in the design of the cam profile. The right side of Figure 7 shows the change from S-NPP, in blue, to JPSS-1 shown in yellow.

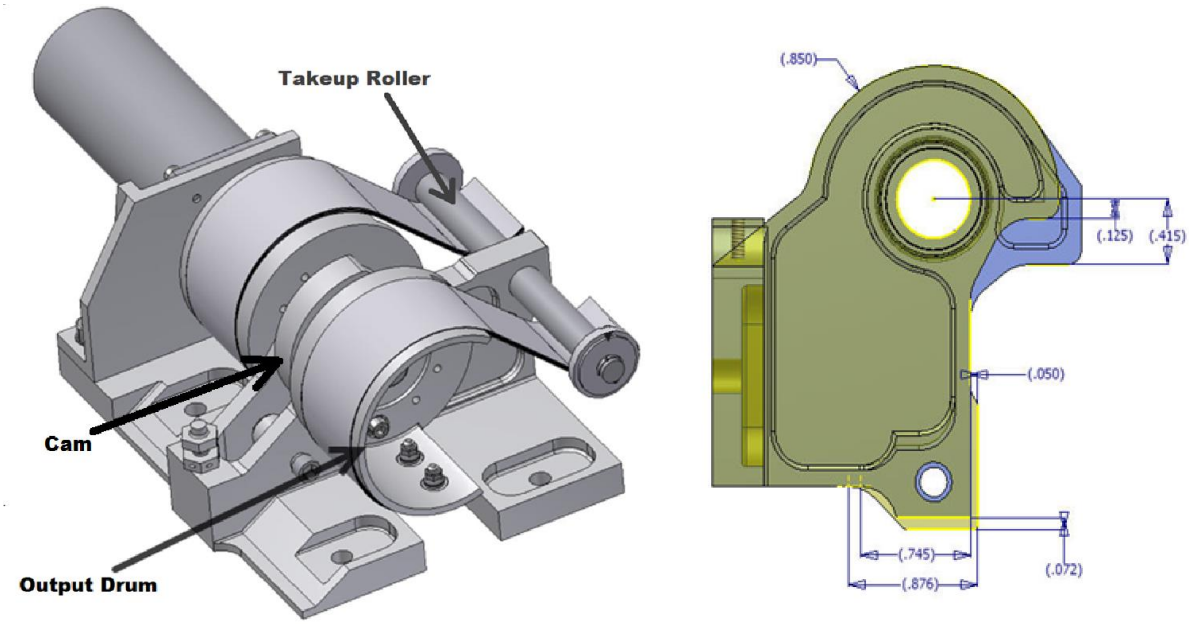

Figure 7. Powered IPH shown in stowed position and Cam profile change (JPSS-1 changes in gold, values in inches)

Figure 8 shows how the previous cam profile resulted in a varying drag due to changes in the compression of the pawl spring across the range of motion. The modification to the cam profile achieved the value associated with the first 110 degrees, and JPSS-1 baseline, also shown in Figure 8. The blue line shows the S-NPP profile and the red line shows the JPSS-1 profile. This change in the cam profile made it consistent with the profile for the MDH, a constant resistive torque profile.

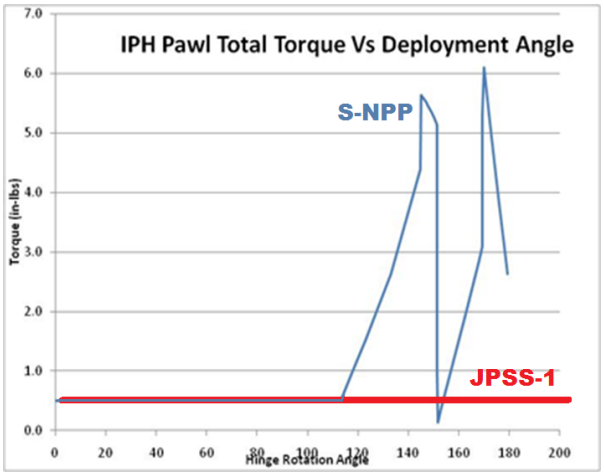

Figure 8. S-NPP variation in pawl drag torque over range of motion

Hinge Testing

The JPSS-1 MDH and IPH were both characterized for sources of drag torque in a much more consistent and repeatable method than S-NPP. Figure 9 shows the test set up used to characterize the MDH hinge. This apparatus consists of a drive motor in-line with a torque sensor and the unit under test. This test drove the hinge in both directions and had the pawls riding on the surface in both directions but did not go through the full range of motion to prevent the pawls from locking out. Figure 9 also shows an example data plot for the MDH hinge resistive torque test. In comparison, S-NPP characterized drag torque manually, with a torque watch and was not as repeatable nor as controllable over the range of travel.

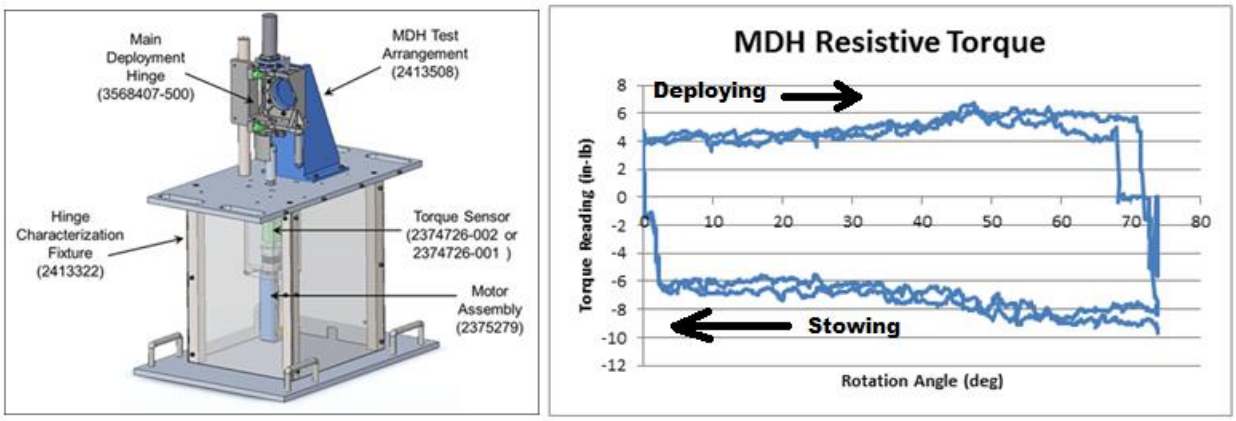

Figure 9. MDH Drag Torque Testing Apparatus and Results

In parallel the harness resistive torque was characterized using a similar apparatus, shown in Figure 10. This apparatus allowed the harness to be articulated over the full 90 degrees in both the deploying and

stowing direction to allow the peak resistive torque to be measured. Measurements are made at ambient, hot, and cold extremes. First the fixture itself is cycled over the thermal environment and driven across the range of motion to characterize the fixture and then testing is repeated once the harness is installed.

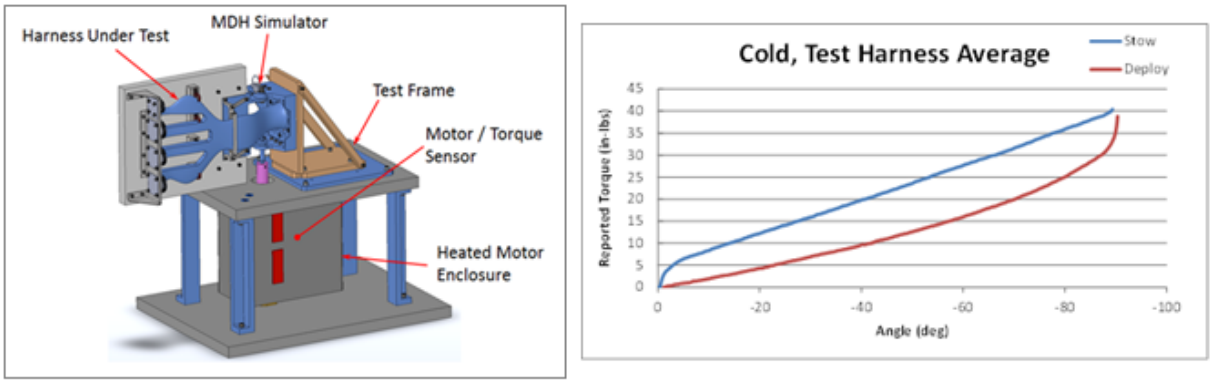

Figure 10 Harness Testing Apparatus and Results

An example data plot on the right side of Figure 10 shows the reduced data to account for the effects of the fixture and the resulting resistive torque of the harness over the range of motion. These results allowed engineering to determine the number springs that were required to meet the torque margin requirements. Once the springs were installed onto the mechanism, it was again attached to the fixture used to characterize the drag torque of the hinge to measure the output of the hinge and to directly measure the output torque of the hinge and validate the torque margin analysis.

Figure 11 shows a typical data plot and the slope of the data shows how the constant torque spring has some variation over the range of motion that the hinge rotates through. The friction in the system due to the applied load of the springs is the difference between the curves divided by two and the output torque of the spring is the average value of the curves. The minimum output torque is considered the available torque to the system for writing torque margin and the minimum value was found to always be at the end of travel.

Figure 11. Typical Torque Data

A similar approach was used to characterize the inter-panel hinges and to determine the number of springs necessary to meet torque margin requirements. Running the hinges through this level of characterization was a significant improvement over the approach taken during the S-NPP effort and provided a high level of confidence in how well the hinges would perform at the solar array subsystem

level. Static proof testing was performed on S-NPP which demonstrated that the design was robust. This step was not completed during the JPSS-1 hinge testing.

Solar Array Subassembly Testing

To be acceptable for delivery to observatory integration, the solar array subsystem had to pass a suite of tests in the sequence shown in Figure 12, which includes procedure numbers for reference only.

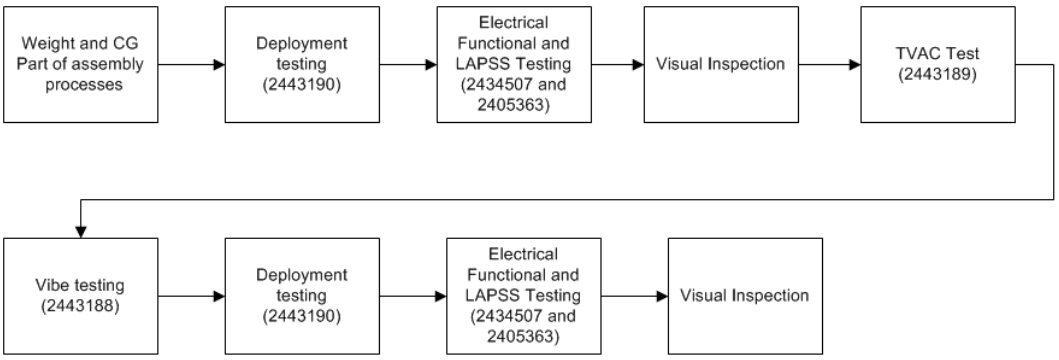

Figure 12: JPSS-1 test flow

Manual deployments were agreed upon at this level of testing since powered deployments were performed at the observatory level pre/post vibration/acoustics testing. Those powered deployments demonstrated the end-to-end capability of the system to power the release mechanism (TiNi actuator) and break the retention bolt.

Deployment testing was a challenge on S-NPP and recognized as a risk during the JPSS-1 program. There were no plans to change the approach in deployments from how S-NPP had done them. It was understood that there were limitations with the air bearing gravity-negation system.

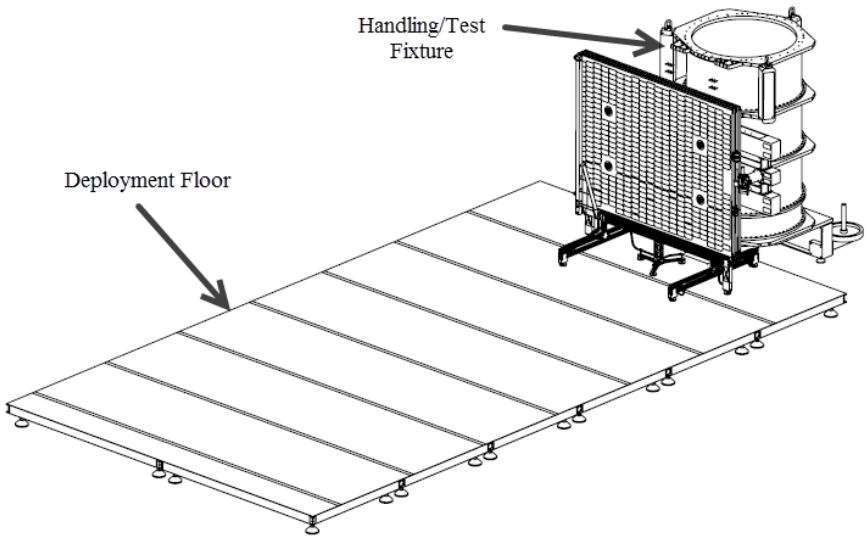

Figure 13 Solar Array Assembly Manual Deployment Test – Stowed Position

During the S-NPP subsystem testing it was not possible to achieve the correct levels during vibration testing and it was deferred to the observatory level. For JPSS-1, a thorough review of the MGSE was

completed and it was decided to create a handling fixture that the array could stay integrated to for deployment, vibration, and thermal testing. This allowed for easier handling and transportation of the entire array, shown in Figure 13.

The deployment floor was aligned to gravity and it was possible to align the main deployment hinge axis to the deployment floor. This was done by placing two laser tracker nests onto the panel and rotating it 90 degrees. The resulting arc measurements allowed the hinge axis orientation to be determined. It was not possible to account for the orientation of the inter panel hinges to the deployment floor. The setup for the alignment of the hinge axis is shown in Figure 14.

During preparation for JPSS-1 deployments, a problem that arose was that the polyolefin membrane roofing material procured would not lay flat and was wavy. This was not acceptable and this cover was discarded in favor of an approach that NASA had developed successfully during the GPM program. That approach consisted of two layers, a layer of Poron™ foam against the deployment floor and a layer of Melinix on top of that. Ball worked with NASA to understand the implementation of this system and it was successfully installed onto the deployment floor. Prior to the first manual deployment run-for-the-record some engineering tests were performed to gain confidence that the deployment would be successful. This was needed as the air bearing offload system was not instrumented to show the amount of load that each air bearing was carrying. The engineering deployments allowed evaluation of the air bearings to determine if they were adjusted correctly and operated over the full range of motion. One thing that was observed was that if an air bearing was overloaded it would “plow” through the poron support and it was easy to note which bearings were not adjusted correctly.

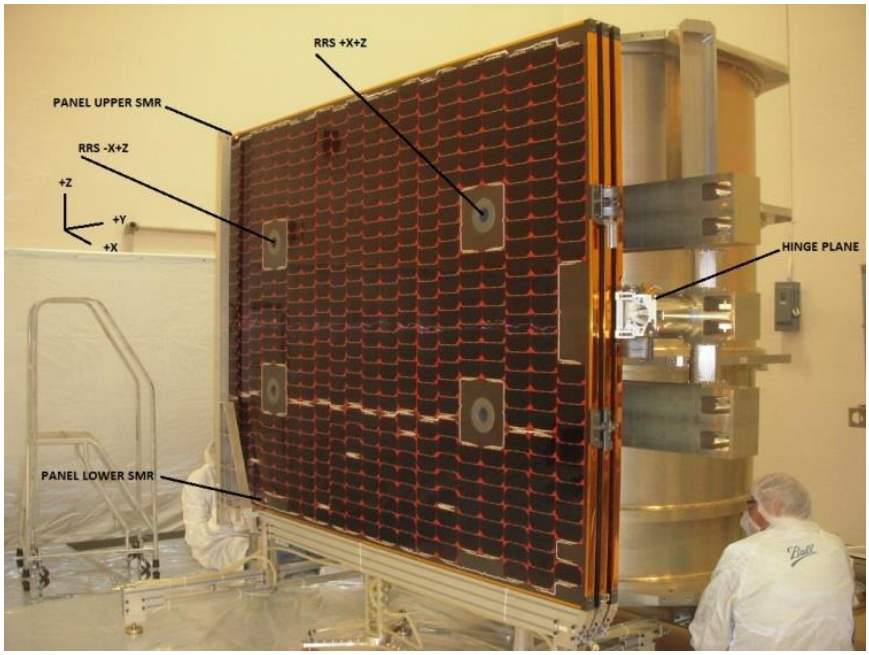

Figure 14. Setup for Alignment of MDH Hinge Axis

The air bearing support was supplied with air through a single hose to each panel and can be seen in Figure 15. It became apparent that the manual handling of these hoses could potentially impact how the array deployed and care had to be taken in how the hoses were managed. If they were twisted the wrong way, then a retarding torque could be applied at the hinge line and impact deployment time or the sequence in which the panels locked out. The first manual deployment took 4 minutes and 30 seconds to complete without requiring intervention.

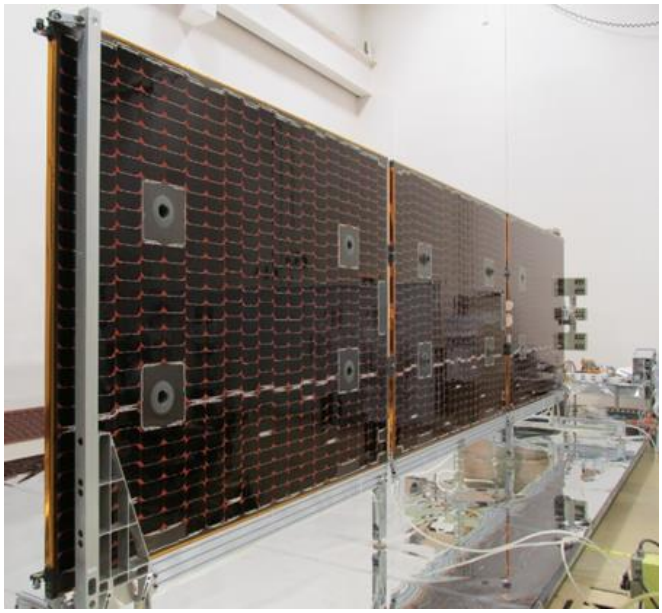

Figure 15. Deployed Array on Air Bearing Support Equipment

After the deployment was completed each hinge line was inspect to verify that the pawls were engaging with the cams correctly. It can be seen in the left-side ovals in Figure 16 that the lower pawl of the MDH engages into the cam further than the upper pawl. This is a result of minor variations in the deployment floor height and the fact that the air bearings cannot be controlled to equally off-load the panel.

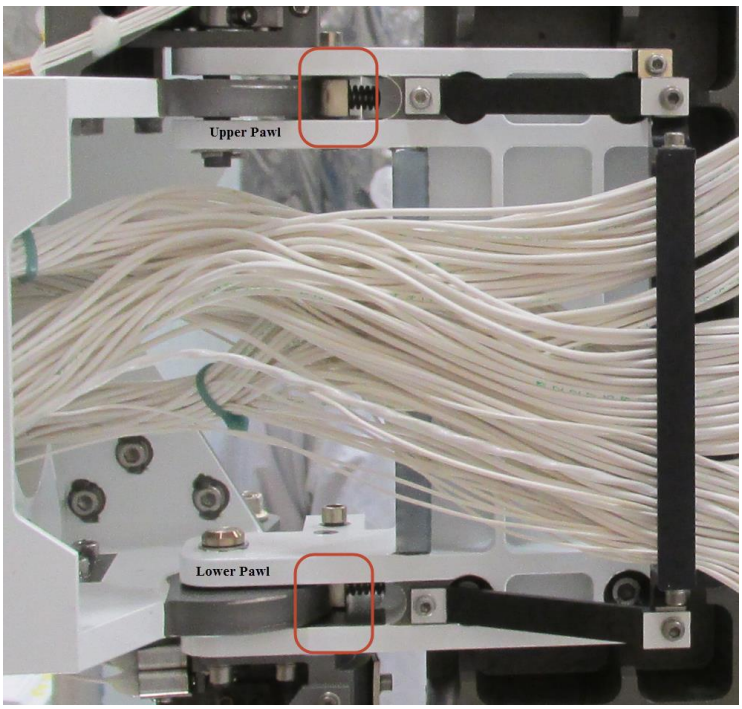

Figure 16. MDH Pawl Engagement Issue

Once the array was in the deployed position it was possible to perform electrical and Large Area Pulsed Solar Simulator (LAPSS) testing. Once the panels were secured in a flight stowed configuration to the MGSE the entire barrel assembly that the array was attached to was transported to perform

environmental testing. Thermal vacuum testing was performed on the entire array for four cycles, to make up for the four cycles missed at the observatory level when the wing is removed from the spacecraft for thermal balance. This test is limited in the ranges to which the array can be exercised. It was not possible to cycle to the hot operational temperature of the array as it would exceed the transition temperature of the shape memory alloy in the TiNi actuators and the limits of the wet lubrication in the eddy current dampers.

The solar array test set up was vibration tested with a solar array mass simulator prior to integration of the flight solar array to the MGSE to validate the modes of the MGSE prior to flight vibration testing. The array was exposed to sine sweep and sine burst to qualify all of the hardware for quasi-static loading and the low-frequency sine transient or sustained sine environments that were anticipated during launch. The test setup is shown in Figure 17. Random vibe was also performed as risk reduction; the array was to be qualified at observatory acoustic testing.

After environmental testing the array was transported back to the deployment floor and configured for manual deployment. With minimal adjustment done to the array and no verification of hinge line orientation the array was deployed and took 9 minutes and 30 seconds to complete. Each panel successfully locked out and completed its range of motion but this significant difference in time could have been an indication of damage to the hardware due to environmental testing. After adjusting the MGSE to orient the handling fixture in a similar manner as the pre-environmental tests it deployed in 5 minutes. This was much more in line with the previous test and, after completing electrical and LAPSS testing, the array was delivered for observatory integration. Once mounted to the satellite bus, the array passed all of its electrical tests.

Figure 17. Solar Array Subsystem Vibration Testing

Satellite Level Testing

At the Observatory level the array was to see more vibration testing, after which first motion testing was required to demonstrate it was going to operate properly after launch. Then, while JPSS-1 was in TVAC testing, the solar array was removed and mounted back to the MGSE and a final full deployment test was

completed. This testing was complicated by the fact that dampers were removed after the array was in the partially deployed condition, after a first motion release, also known as a “pop and catch,” so that the array could be safely stowed to the bus for removal. It was decided to start the deployment test where the pop and catch test had ended to test the dampers thru their full range of motion without adjusting where on the gear train it had stopped. After the array had been attached to the air bearing hardware, the array was deployed. This deployment took longer than anticipated, 10 minutes and 27 seconds, without manual intervention. Without adjusting the test set up, the array was stowed and allowed to deploy from its stowed position again, and that took 8 minutes and 10 seconds, without manual intervention. Since this was still out of family with the subsystem results, an investigation was started to understand the difference. It was determined that since the air bearings were used and adjusted for the observatory-level test, and then utilized untouched for the subsystem level test, they were now improperly adjusted for the subsystem testing. After adjusting the air bearing set up, by manually walking out the array with eddy current dampers removed, the deployment was repeated and completed in 4 minutes and 16 seconds, which matched the results from subsystem level testing. With this success, all that remained before shipment and launch was to remount the array and complete a final pop and catch.

Summary and Lessons Learned

The design and development of the S-NPP array resulted in several lessons learned during the first implementation of this style of array by Ball Aerospace.

- Number of leaf springs used within each drive stack to limit inter-laminar friction.
- Inspection of parts and verification of part processing.
- Cam profile of hinge surfaces to provide constant resistive torque.
- Inadequate resistive torque characterization.
- Inadequate output torque characterization.
- Agreed upon requirements for resistive torque characterization.
- Design of vibe fixtures to achieve required test spectrum.
- Deployment fixturing design and verification.

The JPSS-1 solar array design updates—changing the profile of IPH cam, updates to the constant torque spring and the spring mounting, and removing potential harness hang-ups—and the follow-on tests were very successful, but some issues along the way made it necessary to repeat tests.

- Deployment floor material changes from polyolefin membrane to Poron™ and Melinix.
- Repeatability of MGSE alignment.
- Maintaining configurations of air bearing MGSE between different test set up usage.
- Difficulty repeating air bearing alignments and determining proper offloading.

The issues associated with the air bearings and determining whether the offloading is being accomplished correctly has driven the undertaking of a new research and development effort to address these troubles found during S-NPP and JPSS-1.

Acknowledgements

The authors wish to acknowledge Mr. Joseph Pellicciotti for his crucial support with the S-NPP solar array flight qualification, and for the portions of his presentations which made it into this paper. The authors especially want to thank the engineers, technicians and support personnel of Ball Aerospace who turned the designs into hardware that made these two missions possible.